0026-895X/05/6701-140–151$20.00
MOLECULAR PHARMACOLOGY
Vol. 67, No. 1
3195/1189058
Mol Pharmacol 67:140–151, 2005
Printed in U.S.A.

Amphetamines Take Two to Tango: an Oligomer-Based Counter-Transport Model of Neurotransmitter Transport Explores the Amphetamine Action

Stefan Seidel, Ernst A. Singer, Herwig Just, Hesso Farhan, Petra Scholze, Oliver Kudlacek, Marion Holy, Karl Koppatz, Peter Krivanek, Michael Freissmuth, and Harald H. Sitte

Institute of Pharmacology, Medical University of Vienna, Vienna, Austria

Received December 30, 2003; accepted September 28, 2004

This article is available online at http://molpharm.aspetjournals.org

ABSTRACT

Amphetamine congeners [e.g., 3,4-methylenedioxymetamphetamine (MDMA), or "ecstasy"] are substrates for monoamine transporters (i.e., the transporters for serotonin, norepinephrine, and dopamine); however, their in vivo-action relies on their ability to promote monoamine efflux. The mechanistic basis for this counter transport remains enigmatic. We tested the hypothesis that outward transport is contingent on the oligomeric nature of neurotransmitter transporters by creating a concatemer of the serotonin transporter and the amphetamine-resistant GABA transporter. In cells expressing the concatemer, amphetamine analogs promoted GABA efflux and blunted GABA influx. In contrast, the natural substrates serotonin and GABA only cause mutual inhibition of influx via the other transporter moiety in the concatemer. GABA efflux through the concatemer that was promoted by amphetamine analogs was blocked by the protein kinase C inhibitors GF109203X (bisindoylmaleimide I) and Gö6983 (2-[1-(3-dimethylaminopropyl)-5-methoxyindol-3-yl]-3-(1*H*-indol-3-yl)maleimide). Thus, based on our observations, we propose that, in the presence of amphetamine analogs, monoamine transporters operate as counter-transporters; influx and efflux occur through separate but coupled moieties. Influx and efflux are coupled via changes in the ionic gradients, but these do not suffice to account for the action of amphetamines; the activity of a protein kinase C isoform provides a second stimulus that primes the inward facing conformation for outward transport.

Several characteristics make the three monoamine transporters (for dopamine, serotonin/5-HT, and norepinephrine) of particular medical relevance. 1) Since their seminal discovery in the early 1960s (Axelrod et al., 1961), the norepinephrine and serotonin transporters are considered the prime targets for the most effective antidepressant drugs, which act by blocking transport. 2) Cocaine, which also blocks the dopamine transporter, is notoriously abused for its euphoric and rewarding effects. 3) There is a polymorphism in the promoter region of the serotonin transporter (Lesch et al., 1996); persons that carry the short allele are predisposed to develop depression in response to stressful life events (Lesch et al., 1996; Caspi et al., 2003). 4) A mutation in the norepinephrine transporter causes intracellular retention of the transporter (Hahn et al., 2003) and is associated with postural hypotension in people (Shannon et al., 2000). 5) Finally, amphetamine ("speed") and its congeners, methamphetamine ("ice"), and 3,4-methylenedioxymetamphetamine (MDMA, or "ecstasy"), represent another class of compounds that are abused because of their psychoactive action, which is mediated by their effect on the three monoamine transporters.

Monoamine transporters belong to the superfamily of facilitated transporters. These exploit an ion gradient to translocate the substrate across the membrane bilayer (Henderson, 1993; Torres et al., 2003b). Therefore, depending on the concentration gradients and the net driving force, they are capable of operating in two directions. A model that accounts for the reaction mechanism was formulated some 40 years

This work was supported by grants from the Austrian Science Foundation (FWF) P15034 (to M.F.) and P14509 (to H.H.S.), the "Hygiene"-Fonds of the Vienna University (to H.H.S. and E.A.S.), the Österreichische Nationalbank, project 8514 (to E.A.S.), as well as by a grant ("Epileptosome") from the EU framework program 5.

ABBREVIATIONS: MDMA, 3,4-methylenedioxymetamphetamine; HEK, human embryonic kidney; β-CIT, (1*R*,2*S*,3*S*,5*S*)-3-(4-iodophenyl)-8-[^{3}H]methyl-8-azabicyclo[3.2.1]octane-2-carboxylic acid, methyl ester; hSERT, human serotonin transporter; CFP, cyan fluorescent protein; YFP, yellow fluorescent protein; GFP, green fluorescent protein; FRET, fluorescence resonance energy transfer; PCA, *para*-chloroamphetamine; SERT, serotonin transporter; HPLC, high-performance liquid chromatography; GF109203X, bisindoylmaleimide I; MDMA, 3,4-methylenedioxymetamphetamine; MPP^+, 1-methyl-4-phenylpyridinium; HEK, human embryonic kidney; GAT-1, GABA-tranporter-1; PKC, protein kinase C.

ago (Jardetzky, 1966) and is referred to as the alternate access model: the transporter undergoes a cycle in which the substrate binding site is sequentially exposed; for inward cotransport, the binding site first faces outward to allow for binding of the cotransported ion(s) and substrate. A conformational change ensues that shields the substrate from the extracellular face; the substrate binding site is then accessible from the intracellular face and the cotransported ion(s) and substrate are released, which allows the transporter to adopt the outward-facing conformation. The inward-facing conformation of two bacterial transporters has been visualized with atomic resolution (Abramson et al., 2003; Huang et al., 2003). In conjunction with earlier biochemical experiments, these structures suggest a "rock-and-switch" model that accounts for the conformational cycle: substrate binding is proposed to trigger the switch by lowering the energy barrier between the two conformations. However, the alternate access model does not explain a crucial feature of monoamine transporters: amphetamine analogs induce outward transport of neurotransmitters while they are transported into the cell. This is typically attributed to facilitated exchange diffusion (Fischer and Cho, 1979): amphetamines are thought to induce the accumulation of inward-facing conformations of the transporters; these bind substrate (i.e., the respective neurotransmitter) and extrude it. There are many compelling reasons to question the alternating access model for neurotransmitter transport (Pifl and Singer, 1999; Sitte et al., 2001; Scholze et al., 2002; Adams and DeFelice, 2003) and specifically the model of facilitated exchange-diffusion (Pifl and Singer, 1999; Sitte et al., 2001). In the facilitated exchange diffusion model, for instance, it is not obvious why the inward-facing conformation binds and extrudes the neurotransmitter rather than the amphetamines; upon uptake of amphetamines, they must be present in high concentrations near the transporter. Thus, the locally accumulating amphetamines ought to compete efficiently with substrate for outward transport. We therefore surmised that 1) efflux and influx did not occur sequentially through a monomeric transporter but 2) that they were contemporaneous and thus 3) occurred through distinct moieties within an oligomeric transporter. We tested this hypothesis by creating a concatemer of the (amphetamine-sensitive) serotonin transporter and of the (amphetamine-resistant) GABA transporter. Our observations suggest that the reversal of the ionic gradient(s) does not suffice to support amphetamine-induced transport reversal and identify a prominent role of protein kinase C.

Materials and Methods

Generation of Constructs, Stable Transfection, Cell Culture, and Immunoblotting. Constructs were generated by polymerase chain reaction using appropriate primers (sequence available upon request) as described previously (Schmid et al., 2001; Scholze et al., 2002). These articles also contain a comprehensive list of reagents and their sources. The integrity of the constructs was verified by automated fluorescent chain termination sequencing. The expression vectors were pECFP-C1 or pEYFP-C1 (BD Biosciences Clontech, Palo Alto, CA) which drive the mammalian expression of a fusion protein that comprises the protein of interest fused to cyan or yellow fluorescent protein. HEK293 cells were transfected using the calcium-phosphate coprecipitation method; stable cell clones were selected in the presence of G-418 (Geneticin). Stably transfected cell clones were assessed for binding of the serotonin transporter (SERT) ligand [^{3}H]β-CIT ((1*R*,2*S*,3*S*,5*S*)-3-(4-iodophenyl)-8-[^{3}H]methyl-8-azabicyclo[3.2.1]octane-2-carboxylic acid, methyl ester)). For comparative studies, clones were chosen that expressed similar levels of [^{3}H]β-CIT binding. Electrophysiological experiments were carried out on cells that expressed hSERT in an inducible manner (T-Rex-TetOn; Invitrogen). The expression of cyan fluorescent protein (CFP)- or YFP-tagged proteins was also verified by immunoblotting. Membrane extracts were prepared from HEK293 cells expressing various constructs and from untransfected cells, electrophoretically resolved and transferred to polyvinylidene difluoride membranes. The membranes were probed with an antiserum directed against GFP (BD Biosciences Clontech), which recognizes all fluorescent protein variants (that is GFP, CFP, and YFP); the immunoreactive bands were visualized by using an anti-rabbit antibody conjugated with horseradish peroxidase (Amersham Biosciences, Piscataway, NJ) and enhanced chemiluminescence (reagents from Pierce Chemical, Rockford, IL).

Uptake, Superfusion, and Binding Experiments and Fluorescence Microscopy. The detailed procedures for uptake experiments with radioactively labeled substrates, for superfusion experiments, for binding studies, and for fluorescence microscopy including fluorescence resonance energy transfer (FRET) studies have been described previously (Schmid et al., 2001; Scholze et al., 2002). Uptake of *para*-chloroamphetamine (PCA) was determined as follows: 5×10^5 cells stably expressing SERT were incubated for 1 min at 22°C in Krebs-HEPES buffer (25 mM HEPES, pH adjusted to 7.5 with NaOH) containing 5 mM glucose and concentrations of PCA ranging from 1 to 30 μM in the absence (total uptake) and presence of 1 μM paroxetine (nonspecific uptake). Otherwise, nonspecific uptake by diffusion was defined by employing untransfected cells (which gave comparable results). After 1 min, the medium was aspirated and the cells were rapidly rinsed three times with 1 ml of ice-cold phosphate-buffered saline. Uptake experiments with radiolabeled [^{3}H]serotonin were done in parallel using identical conditions (cells seeded in parallel, same incubation time and washing procedure). Thereafter, PCA was extracted from the cells by addition of 400 μl of acetonitrile. After centrifugation, an aliquot (150 μl) of the supernatant was spiked with internal standard (50 ng of amphetamine) and 6.25 μg of dansyl chloride (Serva Feinbiochemika, Heidelberg, Germany) and mixed with 150 μl of aqueous solution (pH 9.2; final concentration, 15 mM Na_2HPO_4). After 20 min at 65°C, the samples were centrifuged to remove precipitated material; 150 μl was injected into an HPLC system and resolved at a flow rate of 1 ml/min at 50°C (mobile phase, 1:1; 30 mM KH_2PO_4, pH 6:acetonitrile; column, Hewlett-Packard Hypersil MOS 200 $\times$ 2.1 mm; fluorescence detection, Shimadzu RF-551; excitation and emission wavelength, 318 and 510 nm, respectively). The protein kinase C inhibitors GF109203X (bisindoylmaleimide I) and Gö6983 (2-[1-(3-dimethylaminopropyl)-5-methoxyindol-3-yl]-3-(1*H*-indol-3-yl)maleimide) were obtained from Calbiochem and were employed at 1 and 0.5 μM, respectively.

Electrophysiological Experiments. Whole-cell patch-clamp recordings were done on T-Rex-TetOn cells stably expressing the wild-type hSERT under conditions described previously (Sitte et al., 1998). In brief, the holding potential was -70 mV, the inner pipette solution contained KCl, inward (Na^+) currents were elicited by superfusion of the cells with the indicated concentrations of serotonin (5-HT), PCA, 3,4-methylenedioxymetamphetamine (MDMA), and other analogs in the absence and presence of 1 μM paroxetine.

Results and Discussion

Bell-Shaped Concentration Response Curve for Amphetamine-Induced Transport Reversal. In vivo, neurotransmitter transporters form constitutive oligomers (Hastrup et al., 2001, 2003; Schmid et al., 2001; Scholze et al., 2002; Sorkina et al., 2003; Torres et al., 2003a). We hypoth-

esized that the amphetamine-induced outward transport is contingent on the oligomeric nature of the transporter (Fig. 1A); amphetamine binding to one transporter moiety triggers the inward-facing conformation in the adjacent transporter molecule, which extrudes the intracellular substrate. In this model, if all transporters are liganded with amphetamine, transport reversal obviously ought to subside. Thus, this oligomer-based, counter-transport model predicts that amphetamine congeners induce transport reversal with a bell-shaped concentration-response curve. We tested this prediction by employing HEK293 cells that stably expressed the serotonin transporter. The experiments depicted in Fig. 1, B and C, were done with a construct in which the SERT moiety was tagged on its amino and carboxyl termini with cyan and yellow fluorescent protein, respectively (Just et al., 2004). Thus the amino and carboxyl termini were not accessible, similar to the concatemer employed subsequently (see below). We stress, however, that similar results were obtained with an unmodified version of SERT (see also Schmid et al., 2001). The cells were preloaded with the charged substrate [^{3}H]MPP$^+$ and subsequently superfused with PCA; if PCA was employed at a low concentration (Fig. 1B, ■, 3 μM), the compound caused a pronounced efflux of the preloaded substrate [^{3}H]MPP$^+$. As is evident from the concentration-response curve shown in Fig. 1C, concentrations exceeding 3 μM were not more effective; in fact, at saturating PCA concentrations, [^{3}H]MPP$^+$ efflux returned to baseline levels (see also Fig. 1B, open symbols corresponding to superfusion with 1 mM PCA), similar to observations reported for rat hippocampal synaptosomes (Gobbi et al., 2002). The bell-shaped concentration response curve was adequately fitted to an equation for the sum of two opposing processes according to the law of mass action, yielding EC_{50} values of 0.6 ± 0.2 and 87 ± 12 μM for the ascending and descending limbs, respectively. If the superfusion was switched to buffer (Fig. 1B, time = 10 min), the effect of 3 μM PCA gradually subsided as anticipated. By contrast, if PCA was employed at the high concentration of 1 mM, it failed to cause release. Switching to buffer (i.e., removal of PCA by superfusion) triggered a pronounced efflux of [^{3}H]MPP$^+$ (Fig. 1B, □). Thus, a minimum occupancy of transporters by PCA was required to drive efflux, but full occupancy prevented efflux.

In these release experiments, we employed [^{3}H]MPP$^+$ as the substrate; because of its fixed charge, [^{3}H]MPP$^+$ is less prone to diffusion over the cell membrane than [^{3}H]serotonin. Thus, the signal-to-noise ratio is more robust in release experiments done with [^{3}H]MPP$^+$. However, similar observations were made if cells were preloaded with [^{3}H]serotonin; that is, at a high concentration of PCA, release of [^{3}H]serotonin returned to baseline, and release was induced upon washout of PCA (Fig. 1D, open symbols), resulting in a bell-shaped concentration-response curve (Fig. 1E). In contrast, the natural substrate serotonin only promoted efflux of [^{3}H]MPP$^+$, regardless of whether employed at a low concentration (Fig. 1F, 3 μM, closed symbols) or a high concentration (Fig. 1G, 1 mM, open symbols). Most importantly and by contrast with PCA (compare Fig. 1B), switching to buffer caused no increase [^{3}H]MPP$^+$ release after superfusion with 1 mM serotonin (Fig. 1F). Therefore, the concentration-response curve for serotonin was monophasic (Fig. 1G).

Biphasic concentration-response curves have also been noted for amphetamine and tyramine when tested on the noradrenaline release in the rat vas deferens, and these have been proposed to arise from the lipophilic nature of the compounds. Amphetamine may diffuse into the cell and compete for outward transport of noradrenaline (Langeloh et al., 1987). However, the descending limb of the concentration-response curve was only seen at excessive concentrations ($IC_{50} \geq 1$ mM; Langeloh et al., 1987). We tested MDMA, a compound that is substantially more hydrophilic than PCA. The logP values (HyperChem) are −0.32 and 1.07 for MDMA and PCA, respectively; in other words, MDMA is 20-fold more likely to be in the aqueous phase than PCA. Nevertheless, MDMA also failed to elicit release at high concentrations, and washout of MDMA resulted in release of [^{3}H]MPP$^+$ (Fig. 1H). Therefore, the concentration-response curve was adequately described by the sum of two opposing hyperbolas (Fig. 1I); the EC_{50} values were 1.8 ± 0.7 and 131 ± 53 μM for the ascending and descending limbs, respectively. Given that the EC_{50} for the descending limb was within the range calculated for PCA, it seems unlikely that the bell-shaped nature of the concentration-response curve can be solely ascribed to the lipophilic nature of PCA. Finally, serotonin is also lipophilic, and at high concentrations, substantial amounts of serotonin can diffuse through the cell membrane (Scholze et al., 2001; Adams and DeFelice, 2003). Thus, background diffusion per se cannot account for the difference between the action of serotonin and amphetamines.

We have assessed whether the difference between serotonin and PCA can be accounted for by differences in transport velocity (Fig. 2A) and in transport-associated current (Fig. 2D). It is evident from Fig. 2A that the V_{max} values for cellular uptake of serotonin and of PCA were comparable in magnitude (V_{max} = 351 ± 27 and 390 ± 77 pmol/min/10^6 cells and K_M = 3.7 ± 0.9 and 5.0 ± 2.9 μM for serotonin and PCA, respectively). The intracellular water space of 10^6 HEK293 cells has been determined previously to be ~1.3 μl (Sitte et al., 2001); thus, within a minute, PCA and serotonin accumulated to intracellular concentrations of ~300 and 270 μM, respectively. The ability of compounds to promote outward transport is related to their capacity to induce a Na^+ inward current through the dopamine transporter (Sitte et al., 1998; Khoshbouei et al., 2003), and the resulting local accumulation of Na^+ has been directly visualized in response to amphetamine (Khoshbouei et al., 2003). The current traces depicted in Fig. 2B show representative related data for SERT: the inward (Na^+) current observed in the presence of serotonin (purple trace) deactivated rapidly upon removal of the substrate. In contrast, the PCA-induced current (blue trace) faded slowly. This delayed deactivation was also seen with MDMA (yellow trace), albeit to a lesser extent. However, the currents measured in the presence of serotonin, MDMA, and PCA were similar in magnitude. D-Amphetamine has a lower affinity for SERT; therefore, the current induced by 10 μM D-amphetamine (green trace) was lower in magnitude. Deactivation, however, was rapid. Thus, the rate of deactivation was not related to the lipophilic nature of the compounds (because D-amphetamine and PCA are substantially more lipophilic than MDMA).

Two conclusions can be drawn from these observations: 1) the bell-shaped concentration response-curve for PCA is in agreement with our double-barrel model depicted in Fig. 1A. Alternative explanations for the bell-shaped curve in Fig. 1C and the paradoxical efflux caused by superfusion with buffer

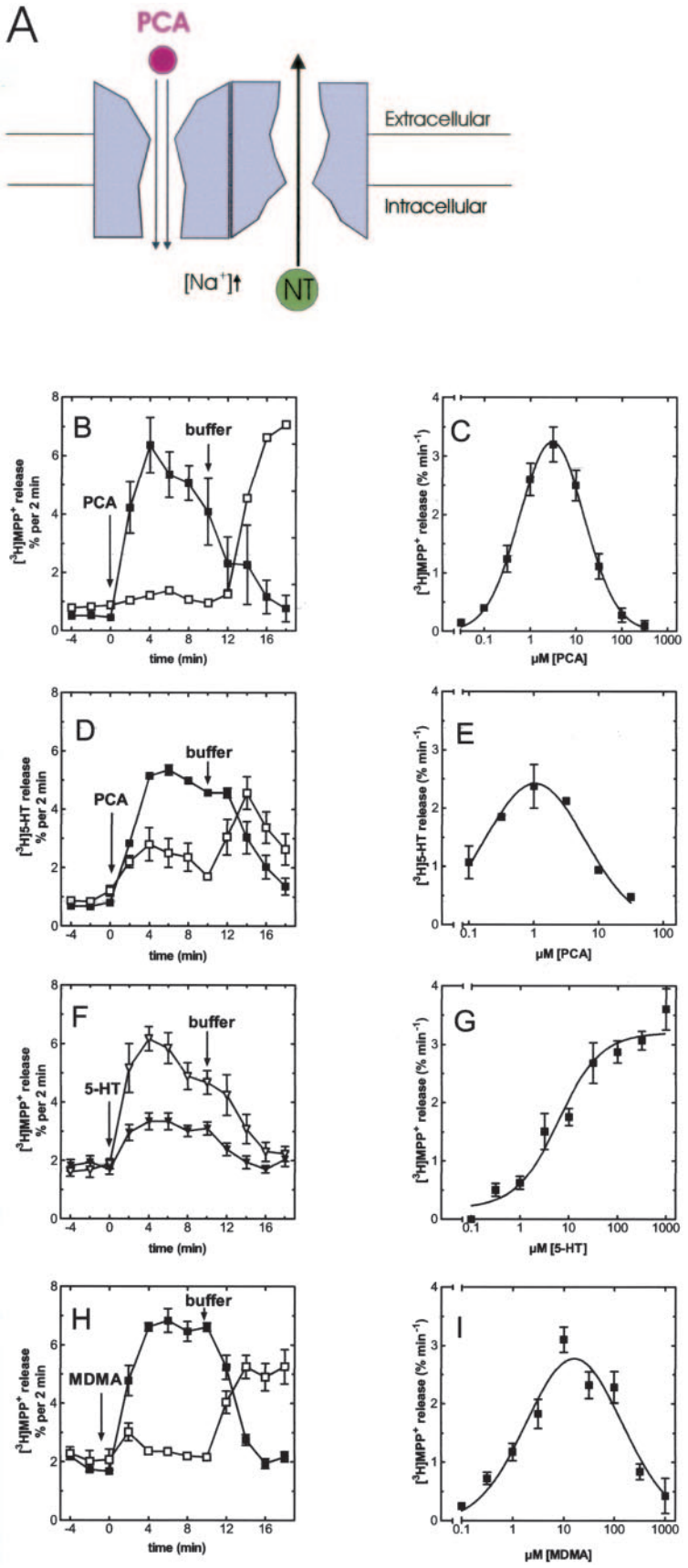

Fig. 1. A, illustration of the oligomer-based counter-transport model in which influx and efflux pathway are separate but contained within the oligomeric quaternary structure of the monoamine transporter. Na^+ influx promoted by the uncoupled current induced by amphetamine analogs (here PCA) provides the driving force for the counter-transport; it promotes the inward-facing conformation that extrudes substrate (here 5-HT). B and C, PCA-promoted [^{3}H]MPP^+ efflux from preloaded HEK293 cells that stably expressed CFP-SERT-YFP. HEK293 cells stably expressing CFP-SERT-YFP (2.5×10^4 cells/cover slip) were preloaded with [^{3}H]MPP^+ (0.2 μM, 20 min, 37°C), transferred to superfusion chambers and superfused with buffer (0.7 ml/min at 22°C). After a washout period of 45 min, fractions (2 min) were collected. After three baseline fractions, at time = 0 min, cells were exposed to 3 μM (■) or 1 mM (□) PCA, and five fractions were collected. Then (time point indicated by arrow), the superfusion was switched to (PCA-free) buffer (four fractions). The release of [^{3}H]MPP^+ is expressed as fractional rate [i.e., radioactivity of a given fraction is expressed as percentage of the radioactivity present in the cells at the beginning of that fraction; for additional details, see Sitte et al. (2001)]. C summarizes the concentration response curves generated as shown in B. PCA-induced [^{3}H]MPP^+ release was defined as the mean of the rates of the three plateau fractions (minutes 4 to 10) minus the mean of the rates of the three basal fractions (minutes −6 to 0). Data represent mean ± S.E.M. of four to six independent experiments carried out in triplicate. D and E, PCA-promoted [^{3}H]5-HT efflux from preloaded HEK293 cells that stably expressed CFP-SERT-YFP. HEK293 cells stably expressing CFP-SERT-YFP (2.5×10^4 cells/cover slip) were preloaded with [^{3}H]5-HT (0.3 μM, 20 min, 37°C), and superfused as in described for B. After three baseline fractions, at time = 0 min, cells were exposed to 3 μM (■) or 1 mM (□) PCA, and five fractions were collected. Then (time point indicated by arrow), the superfusion was switched to (PCA-free) buffer (four fractions). E summarizes the concentration response curves generated as shown in D. PCA-induced [^{3}H]5-HT release was defined as the mean of the rates of the three plateau fractions (minutes 4 to 10) minus the mean of the rates of the three basal fractions (minutes −6 to 0). Data represent mean ± S.E.M. of three to four independent experiments carried out in triplicate. F and G, 5-HT induced [^{3}H]MPP^+ efflux from preloaded HEK293 cells that stably expressed CFP-SERT-YFP. HEK293 cells stably expressing CFP-SERT-YFP were preloaded and superfused as given in B and C. 5-HT was used for induction of efflux; representative traces are shown in B employing 3 μM 5-HT (▲) or 1 mM 5-HT (△). G summarizes the concentration-response curves generated as shown in D. Data represent mean ± S.E.M. of four to six independent experiments carried out in triplicate. H and I, MDMA-promoted [^{3}H]MPP^+ efflux from preloaded HEK293 cells that stably expressed CFP-SERT-YFP. HEK293 cells stably expressing CFP-SERT-YFP (2.5×10^4 cells/cover slip) were preloaded with [^{3}H]MPP^+ as described for B. After three baseline fractions, at time = 0 min, cells were exposed to 3 μM (■) or 1 mM (□) MDMA, and five fractions were collected. Then (time point indicated by arrow), the superfusion was switched to (MDMA-free) buffer (4 fractions). I summarizes the concentration response curves generated as shown in H. Data represent mean ± S.E.M. of four to six independent experiments carried out in triplicate.

(Fig. 1B) include the assumption that the increasing internal concentration of PCA may progressively compete with labeled substrate for internal binding and efflux, and this ought to result in a biphasic curve. However, this interpretation fails to explain why the concentration-response curve for serotonin is not bell-shaped. 2) The localized accumulation of Na^+ on the intracellular side plays a crucial role in our model because it provides the driving force (Fig. 1A). A rise in the internal Na^+ concentration clearly cannot suffice to explain the differences between amphetamines and the natural substrate serotonin, because both PCA and serotonin are taken up at comparable rates and induce currents of similar size. The delayed deactivation of the current in the presence of PCA suggests a long-lasting modification of the transporter channel but cannot per se account for the difference in efflux.

Concatemerization of SERT and GAT-1. Our model (Fig. 1A) assumes that efflux and influx pathways are through separate transporter molecules that are contained within an oligomer. Thus, a monomeric transporter ought to be resistant to amphetamine-induced transport reversal. This prediction, however, cannot be tested because monomeric transporters are retained within the cell (Scholze et al., 2002; Sitte and Freissmuth, 2003). As an alternative, we generated a transporter concatemer by fusing a monoamine transporter to a partner that was insensitive to the action of amphetamine analogs. Of the several combinations that were tried, only the concatemer (Fig. 3A, schematic rendering) composed of the SERT and of the GABA-tranporter-1 (GAT-1) mediated cellular uptake of substrates. The concatemer was tagged on its amino terminus with CFP, which afforded the visualization by fluorescence microscopy (Fig.

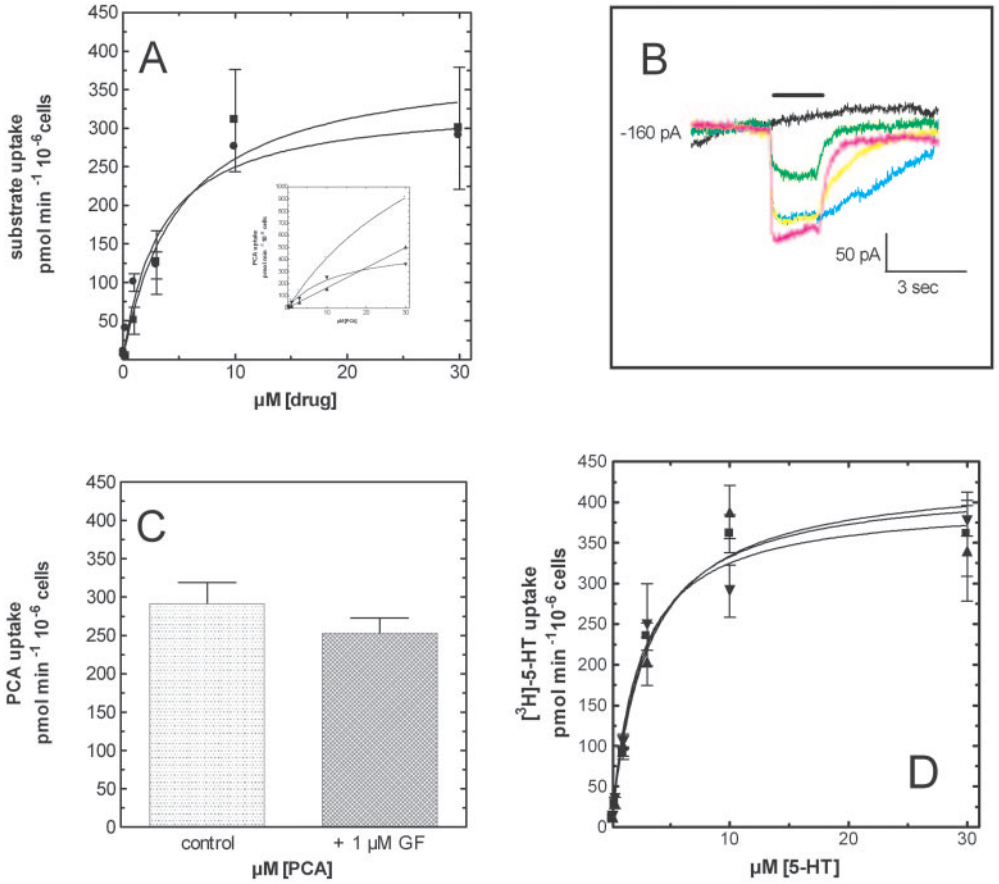

Fig. 2. A, saturation uptake curves of [^{3}H]5-HT and PCA in HEK293 cells that stably expressed the wild-type SERT. Uptake assays were performed in 35-mm tissue culture dishes at a cell density of 5×10^5 cells per dish, seeded the day before the experiment. Cells were incubated in a final volume of 1 ml with the indicated concentrations of [^{3}H]5-HT (●) or PCA (■) for 1 min. Uptake was terminated by rapid removal of substrate-containing buffer and three rapid washes with ice-cold buffer. Nonspecific uptake (measured in the presence of 1 μM paroxetine) was subtracted. In case of [^{3}H]5-HT, the remaining content of radiolabel was determined by cell lysis with 1% SDS and subsequent conventional scintillation counting. PCA-uptake was determined by HPLC as outlined under *Materials and Methods*. The symbols represent mean ± S.E.M. of three and four experiments (for [^{3}H]5-HT and PCA, respectively) carried out in triplicate. The inset shows a representative example of PCA-uptake curves ([squares], total uptake; △, nonspecific uptake; and ▽, resulting specific uptake). B, whole-cell patch-clamp recordings of a T-Rex-TetOn cell stably expressing the wild-type hSERT. The holding potential was −70 mV and the dotted line denotes the zero current; the solution used to fill the patch pipette contained KCl. The bar indicates superfusion with 30 μM 5-HT in the absence (purple trace) and presence (black trace) of 1 μM paroxetine or 10 μM PCA (blue trace), 10 μM MDMA (yellow trace), and 10 μM D-amphetamine (green trace). C and D, effect of protein kinase C inhibitors on cellular uptake of PCA (C) and of [^{3}H]serotonin (D). HEK293 cells stably expressing CFP-hSERT-YFP (5×10^5 cells/well) were incubated in a final volume of 1 ml containing 30 μM PCA in the absence (left bar) and presence of 1 μM GF109203X (right bar; $p = 0.16$) for 1 min at 22°C. Nonspecific uptake was measured in the presence of 1 μM paroxetine. PCA uptake was determined by HPLC as outlined for A. The symbols represent mean ± S.E.M.; the difference between the absence and presence of GF109203X was not statistically significant ($p = 0.17$, Student's t test; $n = 12$). D, HEK293 cells stably expressing CFP-hSERT-YFP (1×10^5 cells/well) were incubated in a final volume of 0.1 ml containing the indicated concentrations of [^{3}H]5-HT the absence (■) or presence (▲) of 1 μM GF109203X and presence of 1 μM Gö 6983 (▼) for 1 min at 22°C. Nonspecific uptake (measured in the presence of 1 μM paroxetine) was less than 10% and was subtracted. The symbols represent mean ± S.E.M. of three experiments carried out in triplicate.

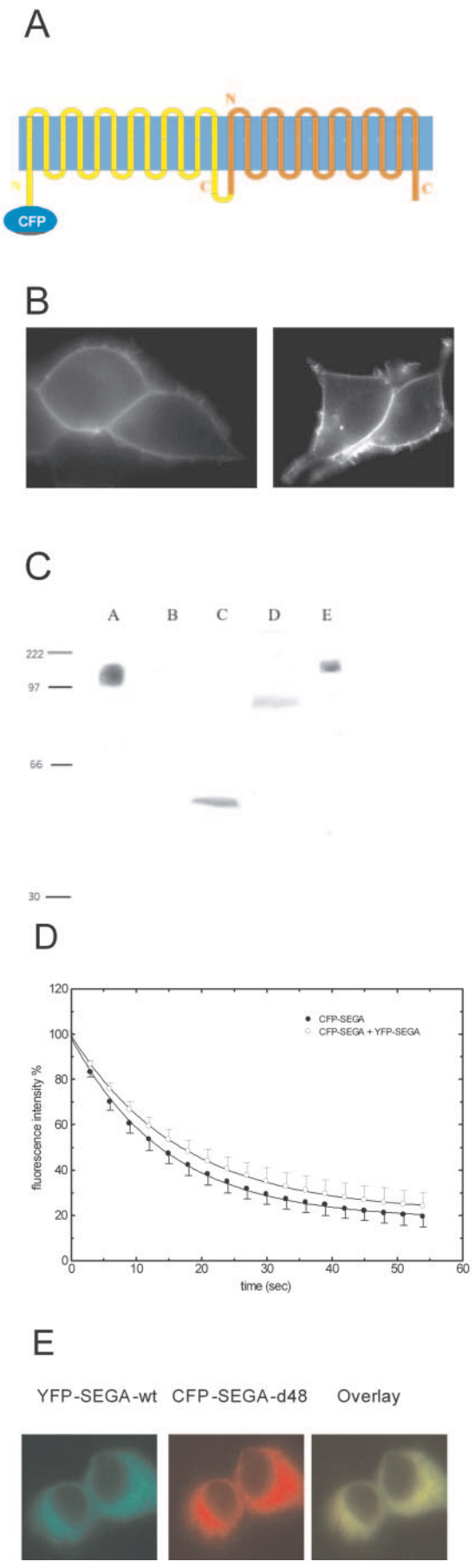

3B, right).In all other instances, concatemers were retained within the cell. As a control, we employed a dually tagged CFP-SERT-YFP, in which (similar to the SERT moiety in the concatemer) both the amino and carboxyl termini are masked by an additional protein. Nevertheless, CFP-SERT-YFP is also expressed at the cell surface (Fig. 2B, left) (for detailed characterization, see Just et al., 2004). We verified by immunoblotting that CFP-SERT-GAT-1 was expressed as an intact protein. CFP-SERT-GAT-1 migrated as a broad band in the range of 150 to 160 kDa (Fig. 3C, lane A), which is in a manner consistent with its glycoprotein nature and with its expected molecular weight. This band was absent in untransfected cells (lane B) and comparable in size to a concatemer formed by YFP fused to two GAT-1 moieties (lane E). It was noteworthy that lane A did not contain any additional immunoreactive material in the range where YFP-GAT-1 (compare lane D) or a fragment comprising the first six transmembrane helices of the SERT fused to YFP (compare lane C) or YFP (~30 kDa) migrated. Thus, the vast majority of the concatemer was expressed as an intact fusion protein. Neurotransmitter transporters exist in oligomeric complexes of higher order, the minimum size being a tetramer (Hastrup et al., 2003; Just et al., 2004). Despite the steric hindrance, a concatemer ought to still allow for the formation of a tetrameric structure (i.e., a dimer of dimers). This conjecture was tested for the SERT moiety by employing CFP- and YFP-tagged versions of the concatemer. The oligomeric nature of the concatemers was directly visualized in living cells using FRET (Fig. 3D). It is not possible to carry out a similar experiment with the GAT-1 moiety, because GAT-1 does not tolerate a tag on the carboxyl terminus; an intact free carboxyl terminus is required for export of GAT-1 from the

Fig. 3. A, schematic rendering of the CFP-SERT-GAT-1 concatemer consisting of the hSERT and the rat GAT-1 tagged with CFP at the N terminus of the hSERT. B, visualization of transporter molecules by fluorescence microscopy. HEK293 cells were transfected with a vector coding for CFP-SERT-YFP (left) or for CFP-SERT-GAT-1 (right). The next day, the fluorescent proteins were visualized (63×, oil immersion) using a CFP filter set (wavelengths: for excitation, 440 nm; dichroic mirror, 455 nm; emission, 480 nm). Images are representative of two to five transfections each (with 5 to 12 images/transfection). C, detection of CFP- or YFP-tagged transporters by immunoblotting. Membrane extracts (30 μg/lane) were prepared from HEK293 cells expressing CFP-SERT-GAT-1 (A), untransfected HEK293 cells (B), a carboxyl terminal fragment comprising the first six transmembrane helices of SERT fused to CFP (C), YFP-GAT-1 (D), and the concatemer YFP-GAT-1-GAT-1 (E), electrophoretically resolved and transferred to polyvinylidene difluoride membranes that were probed with an antiserum directed against GFP; the immunoreactive bands were visualized with the use of enhanced chemoluminescence. Two additional experiments gave similar results. D, donor photobleaching curves for CFP-SERT-GAT-1 in the absence and presence of YFP-SERT-GAT-1. The lifetime of fluorescence was determined in cells that expressed only the donor CFP-SERT-GAT-1 (●) or the donor (i.e., CFP-SERT-GAT-1) and the acceptor YFP-SERT-GAT-1 (○). The procedures of FRET microscopy (including filter sets and lamp intensity for bleaching, image capture, and digitization as well as quantification by the MetaFluor Software package) are described in detail elsewhere (Scholze et al., 2002). Donor fluorescence decay curves were recorded over nine different cells, normalized to the fluorescence recorded at time = 0 and averaged; error bars indicate S.D. Time constants for HEK293 cells transfected with CFP-SERT-GAT-1 ($\tau = 14.3 \pm 2.2$ s) and cotransfected (CFP-SERT-GAT-1 + YFP-SERT-GAT-1) HEK293 cells ($\tau = 20.5 \pm 5.6$ s) were significantly different ($p < 0.01$; t test for unpaired data). E, HEK293 cells were transiently transfected with YFP-tagged wild-type SEGA (YFP-SEGA-wt, red) and CFP-tagged SEGA lacking the last 48 amino acids (CFP-SEGA-d48, green). The fluorophores were visualized 24 h later using the appropriate filter sets. Both images were overlaid using the MetaMorph software.

endoplasmic reticulum (Farhan et al., 2004). As an alternative, we therefore used a retention assay; if the carboxyl terminus of GAT-1 is removed, the resulting truncated transporter acts in a dominant-negative manner by retaining the wild-type transporter in the endoplasmic reticulum (Farhan et al., 2004). Hence, we created a CFP-SERT-GAT-1 in which the entire carboxyl terminus was removed (Fig. 3E, CFP-SEGA-d48) and coexpressed this protein with YFP-tagged SERT-GAT-1; as is evident from Fig. 3E, middle, the truncated concatemer was retained within the cell and, most importantly, efficiently prevented the intact concatemer from reaching the cell surface (Fig. 3E, left; the right shows the optical overlay that documents a perfect colocalization). We therefore conclude that each moiety in the concatemer can form contacts with its counterpart in a neighboring concatemer; in other words, the concatemers form dimers (and possibly larger complexes). However, we stress that we do not have any evidence for a direct interaction (or conformational coupling) between SERT and GAT1 in this concatemer.

The pharmacological characterization showed that the fusion of the two transporters did not substantially alter the functional properties of each individual moiety; this was evaluated by uptake of [^{3}H]GABA (Fig. 4A; K_M = 5.7 ± 1.7 and 5.3 ± 0.7 μM; V_{max} = 463 ± 47 and 364 ± 15 pmol/min/10^{-6} cells for YFP-GAT-1 and CFP-SERT-GAT-1, respectively) and of [^{3}H]5-HT (Fig. 4B; K_M = 2.5 ± 0.7 and 4.0 ± 1.7 μM; V_{max} = 241 ± 20 and 202 ± 29 pmol/min/10^{-6} cells for CFP-SERT-YFP and CFP-SERT-GAT-1, respectively). The most pronounced change was a modest decline in the affinity of the SERT inhibitor [^{3}H]β-CIT (Fig. 4C; B_{max} = 1.4 ± 0.1 and 1.5 ± 0.1 pmol/mg; K_D = 0.8 ± 0.1 and 1.9 ± 0.4 nM for CFP-SERT-YFP and CFP-SERT-GAT-1, respectively). A modest (~ 2-fold) reduction in affinity was also seen in inhibition experiments (uptake and binding challenged by various substrates and blockers; data not shown).

Influx of Na^+ and Cross-Inhibition of GAT-1. SERT and GAT-1 differ in their Na^+ requirement; first, one Na^+ ion is thought to be cotransported with serotonin by SERT, whereas GABA uptake is associated with the uptake of two Na^+ ions (Rudnick, 1998; Chen et al., 2004). Second, GAT-1-dependent uptake requires higher concentrations of extracellular Na^+. This was also seen in the concatemer (Fig. 5), with half-maximum stimulation occurring at 15 ± 8 and >54 ± 10 mM extracellular Na^+ for SERT and GAT-1, respectively. We stress that the curve in Fig. 5 covers only the range up to 100 mM NaCl to illustrate the difference between the SERT and GAT-1 moiety. However, it was evident that 150 mM NaCl did not suffice to saturate GAT-1 (data not shown); thus, the EC_{50} of >54 ± 10 mM is only a rough estimate. It is noteworthy that these affinity estimates were comparable with those obtained with the wild-type versions of SERT and GAT-1 (data not shown). Thus, each transporter moiety in the concatemer seemed to function independently. This conclusion was also reached in the characterization of a concatemer comprising SERT and the noradrenaline transporter (Horschitz et al., 2003). The localized accumulation of Na^+ on the intracellular side plays a crucial role in our model because it provides the driving force (Fig. 1A). Thus, because of

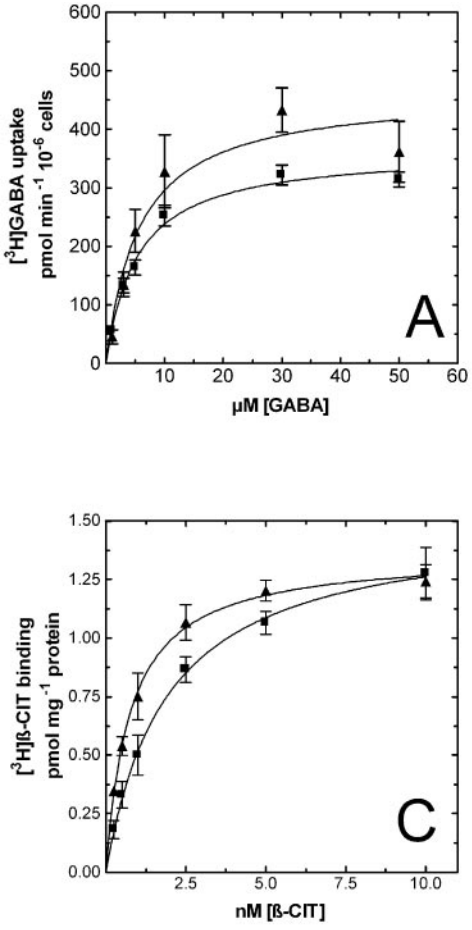

Fig. 4. Saturation curves for uptake mediated by the CFP-SERT-GAT-1 concatemer. HEK293 cells stably expressing CFP-SERT-GAT-1 were plated on 48-well dishes (1×10^5 cells/well). On the next day, cells were incubated in a final volume of 0.1 ml with the indicated concentrations of [^{3}H]GABA for 1 min (A, ■, CFP-SERT-GAT-1 concatemer; ▲, CFP-GAT-1-wt) or of [^{3}H]MPP^+ for 3 min (B, ▲, CFP-SERT-GAT-1 concatemer; ■, CFP-SERT-YFP). Nonspecific uptake (measured in the presence of 10 μM tiagabine and 1 μM paroxetine for the GAT and SERT moieties, respectively) was less than 10% and was subtracted. The symbols represent mean ± S.E.M. of four experiments carried out in triplicate. C, comparative radioligand binding studies to CFP-SERT-YFP and CFP-SERT-GAT-1. Saturation curves for binding of [^{3}H]β-CIT ((1*R*,2*S*,3*S*,5*S*)-3-(4-iodophenyl)-8-[^{3}H]methyl-8-azabicyclo [3.2.1]octane-2-carboxylic acid, methyl ester)). Membranes (30 μg) prepared from HEK293 cells stably expressing CFP-SERT-GAT-1 (■) or CFP-SERT-YFP (▲) were incubated with the indicated concentrations of [^{3}H]β-CIT (specific activity, 64.7 Ci/mmol) in a final volume of 0.5 ml of buffer (20 mM HEPES·NaOH, 1 mM EDTA, and 2 mM $MgCl_2$, pH 7.5) for 1 h at 22°C. Binding was terminated by filtration through glass fiber filters. Nonspecific binding (determined in the presence of 1 μM paroxetine) was <20% at the highest radioligand concentration employed and was subtracted.

the concomitant pronounced influx of Na^+ through the SERT moiety (Fig. 2B, current traces)—and the ensuing local accumulation of Na^+ (Khoshbouei et al., 2003), which diminishes the driving force—we expected amphetamine congeners and serotonin to blunt [^{3}H]GABA uptake by the GAT-1 moiety of the concatemer; by analogy, the presence of GABA is expected to inhibit uptake of serotonin. These predictions have been verified: 1) GABA decreased the maximum velocity (V_{max}) of serotonin uptake by about 50% (Fig. 5B, K_M = 3.8 ± 0.8 and 2.6 ± 0.8 μM; V_{max} = 238 ± 13 and 118 ± 13 pmol/min/10^{-6} cells in the absence and presence of 10 μM GABA, respectively). 2) Likewise, the maximum velocity of [^{3}H]GABA influx was reduced by PCA (Fig. 4C; K_M = 4.8 ± 0.7 and 4.2 ± 1.1 μM; V_{max} = 320 ± 14 and 226 ± 16 pmol/min/10^{-6} cells in the absence and presence of 10 μM PCA, respectively) and serotonin (Fig. 5D; K_M = 4.2 ± 0.5 and 4.0 ± 06 μM; V_{max} = 172 ± 16 and 102 ± 14 pmol/min/10^{-6} cells in the absence and presence of 10 μM serotonin, respectively). V_{max} under control conditions differs in Fig. 5, C and D, because different stably transfected cell lines were used. 3) Consistent with their ability to induce transporter currents of comparable magnitude (compare Fig. 2B), PCA, MDMA, and serotonin blunted [^{3}H]GABA influx to similar levels at saturating concentrations; that is, maximum inhibition was about 40% (Fig. 5E; IC_{50}: MDMA, 0.36 ± 0.08 μM; PCA, 0.27 ± 0.05 μM; serotonin, 0.36 ± 0.06 μM). In cells

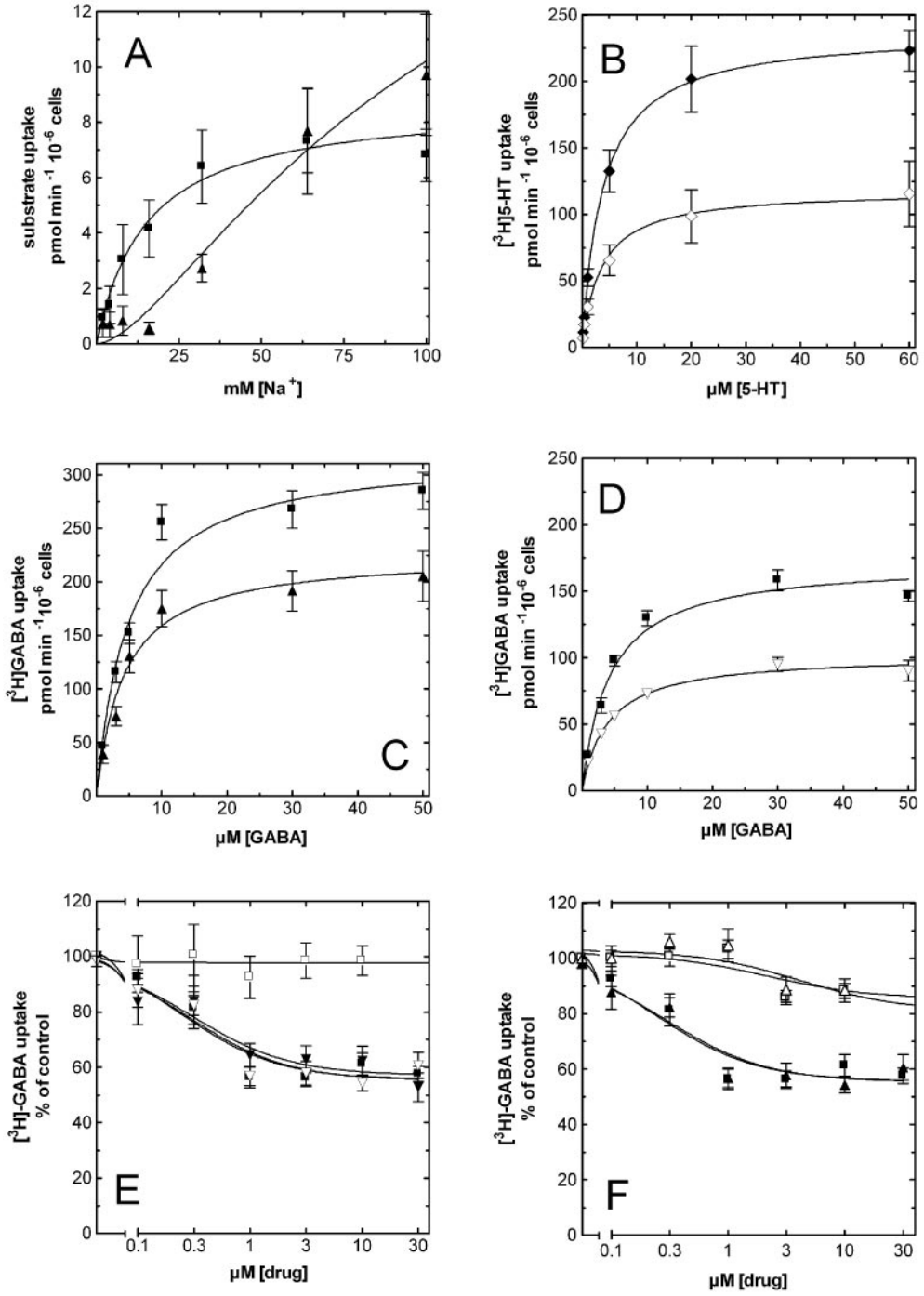

Fig. 5. Na^+ dependence of substrate uptake by the CFP-SERT-GAT-1 concatemer (A) and mutual inhibition of substrate uptake by CFP-SERT-GAT-1 (B–E). A, HEK293 cells (1×10^5 cells/well) stably expressing CFP-SERT-GAT-1 were incubated with [^{3}H]GABA (1.6 μCi/well; specific activity ranging from 85 to 110 Ci/mmol) and 2 μM unlabeled GABA (▲) or [^{3}H]5-HT (2.3 μCi/well; specific activity 21.5 Ci/mmol) and 0.8 μM unlabeled 5-HT (■) with the indicated concentrations of Na^+ for 3 min and 1 min, respectively, in a final volume of 0.1 ml. Iso-osmotic replacement of Na^+ was done by employing choline (as the chloride salt). Nonspecific uptake was measured in the presence of 10 μM tiagabine and 1 μM paroxetine, respectively. B, HEK293 cells stably expressing CFP-SERT-GAT-1 (1×10^5 cells/well) were incubated with the indicated concentrations of [^{3}H]5-HT (2.3 μCi/well) in the absence (♦) and in the presence of 10 μM GABA (◇). C and D, HEK293 cells stably expressing CFP-SERT-GAT-1 were incubated with the indicated concentrations of [^{3}H]GABA (1.6 μCi/well) in the absence (■) or presence of either 10 μM PCA (▲; C) or 10 μM 5-HT (▽; D). E, HEK293 cells stably expressing CFP-SERT-GAT-1 or, as control, YFP-GAT-1 (□), were incubated with [^{3}H]GABA (1.6 μCi/well) and 3 μM unlabeled GABA in the presence of the indicated concentrations of PCA (□ and ■), MDMA (▲), or 5-HT (△). Data represent means ± S.E.M. of five to six experiments carried out in triplicate. F, HEK293 cells were cotransfected to coexpress YFP-GAT-1 and CFP-SERT-YFP (open symbols) were incubated with [^{3}H]GABA (1.6 μCi/well) and 3 μM unlabeled GABA in the presence of the indicated concentrations of PCA (squares) or 5-HT (triangles). The filled symbols represent the corresponding data obtained on HEK293 cells stably expressing CFP-SERT-GAT-1 (from E) and have been added for the sake of direct comparison. Uptake in the absence of compound was 1934 ± 511 cpm and 2125 ± 528 cpm for cells expressing CFP-SERT-GAT1 and for cells coexpressing YFP-GAT-1 and CFP-SERT-YFP, respectively, and this value was 100% to normalize for interassay variation. Data represent means ± S.E.M. of three to four experiments carried out in triplicate.

that solely expressed YFP-GAT-1, the amphetamine analogs had no effect on [^{3}H]GABA uptake (shown for PCA in Fig. 5E, □). Finally, in cells that had been transfected to coexpress SERT and GAT1 as unfused, separate moieties, PCA (Fig. 5F, □) and MDMA (Fig. 5F, △) caused only a modest inhibition (by ~10% at 10 μM). Likewise (and in contrast to cells expressing the concatemer), in these cotransfected cells, GABA did not inhibit influx of [^{3}H]serotonin (data not shown). We note that the IC_{50} (~0.4 μM) of MDMA, PCA, and serotonin was substantially lower than their K_M or K_i values. This indicates that a low occupancy of the transporter suffices to elicit Na^+ influx. This interpretation is consistent with the fact that charge movement through the transporter is larger than predicted for a stoichiometrically coupled cotransport (Adams and DeFelice, 2003).

PCA Induces Counter-Transport of GABA in the Concatemer. Because PCA, MDMA, and serotonin blunted [^{3}H]GABA uptake by the concatemer, it was safe to conclude that the local accumulation of Na^+ (Khoshbouei et al., 2003) was sufficient in magnitude to be sensed by the GAT-1-

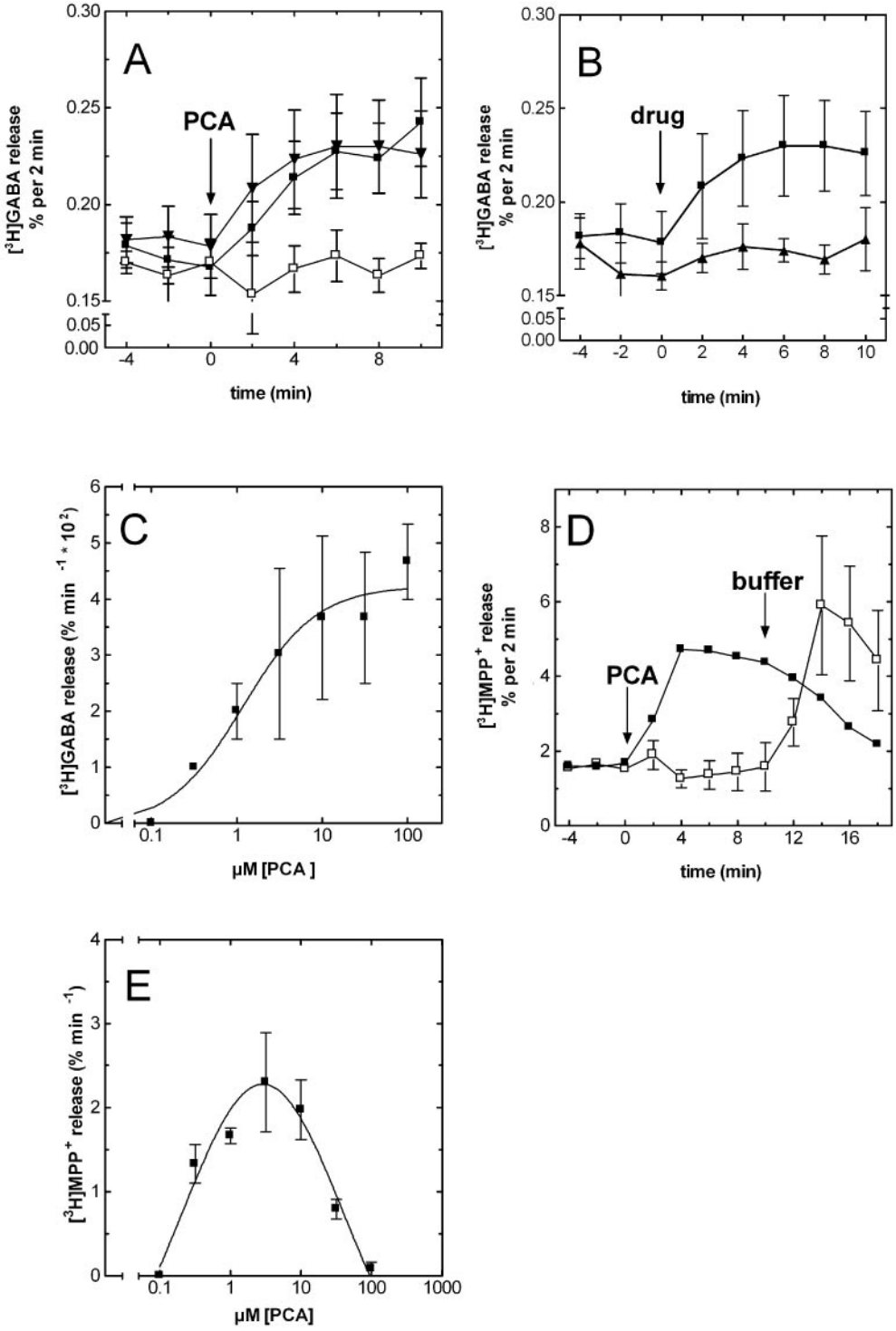

Fig. 6. PCA-induced efflux of [^{3}H]GABA (A–C) and of [^{3}H]MPP^+ (D and E) from HEK293 cells stably expressing CFP-SERT-GAT-1. A, B, and D, time course. HEK293 cells stably expressing CFP-SERT-GAT-1 were preloaded with [^{3}H]GABA (A and B) and [^{3}H]MPP^+ (D) and superfused with buffer as outlined in the legend to Fig. 1B. After three baseline fractions, cells were exposed to different concentrations of PCA or serotonin (A, ■, 10 μM PCA; ▼, 1 mM PCA; □, 1 mM PCA + 10 μM tiagabine; B, ■, 30 μM PCA; ▲, 100 μM 5-HT; D, ■, 3 μM PCA; □, 1 mM PCA) for five fractions. At the time point indicated by the arrow in C, the superfusion was switched to (PCA-free) buffer (four fractions). C and E summarize the corresponding concentration curves derived from experiments analogous to those shown in A and C, respectively. Basal efflux of [^{3}H]GABA was 278 ± 48 cpm; PCA-induced efflux increased to 446 ± 61 cpm. The symbols represent means ± S.E.M. of four independent experiments carried out in triplicate.

moiety despite its low affinity for sodium (compare Fig. 4A). Our oligomer-based counter-transport model (Fig. 1A) predicts that amphetamine analogs ought to trigger outward transport of [^{3}H]GABA by the concatemer. A further prediction concerns the shape of the concentration-response curve; this ought to be monophasic rather than bell-shaped because amphetamine analogs do not block the [^{3}H]GABA efflux pathway (i.e., GAT-1). Both predictions have been verified. PCA triggered efflux of [^{3}H]GABA from preloaded cells (Fig. 6A, ■); this release was not further augmented by raising the concentration of PCA to 1 mM (Fig. 6A, ▲), displaying a concentration-response curve that was adequately described by a rectangular hyperbola based on the law of mass action (Fig. 6C; EC_{50} = 0.9 ± 0.5 μM). PCA-induced [^{3}H]GABA efflux was blocked by the GAT-1 inhibitor tiagabine (Fig. 6A, □). Analogous observations were made with MDMA; finally, [^{3}H]GABA efflux was not observed in the presence of serotonin (Fig. 6B).

PCA also caused efflux of [^{3}H]MPP^+ from preloaded cells that expressed the concatemer (Fig. 5C; 3 μM PCA, ■). Its effects were qualitatively similar to those seen in cells expressing the wild-type version of SERT [that is, 1) outward transport of [^{3}H]MPP^+ was lower at 1 mM than at 3 μM PCA (Fig. 5C, compare □ and ■) and 2) the concentration-response curve was bell-shaped (EC_{50} = 0.3 ± 0.1 and 46 ± 17 μM for the ascending and descending limbs, respectively; compare Fig. 1, B and C, and Fig. 5 C and D, respectively)]. Considering the dimeric model depicted in Fig. 1A, PCA should not trigger any [^{3}H]MPP^+ efflux through the concatemer because the dimeric partner is a GAT-1 moiety. The fact that PCA did nevertheless induce transport reversal also in the SERT moiety may best be explained by the fact that the concatemer also exists as an oligomeric complex (see Fig. 3, D and E). This conjecture is also supported by the following observation: the maximal efflux of [^{3}H]MPP^+ supported by the concatemer was only about 40 to 60% of that mediated by wild-type SERT (compare peaks of the bell-shaped curves in Figs. 1C and 5D), although we employed stably transfected cell clones that expressed comparable levels of SERT (as assessed by binding of the inhibitor [^{3}H]β-CIT; see Fig. 4) and supported comparable influx rates. The steric constraints imposed on an oligomeric concatemer allows us to rationalize the lower maximal efflux that PCA elicits through the SERT moiety of the concatemer. Upon PCA-induced Na^+-influx, there are fewer transporters available to adopt the inward-facing conformation and extrude the substrate; that is, if one assumes the transporters to be tetramers, at 50% occupancy, there would be two transporters available to extrude substrate in wild-type SERT but only one in the concatemer.

Na^+ is dispensable for binding of amphetamine (Schwartz et al., 2003), but Na^+ influx plays a critical role in providing the driving force (Rudnick, 1998; Chen et al., 2004) for transport reversal. However, the transporter that has amphetamine bound is unavailable for outward transport. Thus, based on the available data, we conclude that the action of amphetamine analogs is contingent on a separate influx and efflux pathway, which are contained within an oligomer. It is surprising that we have been unable to detect any outward transport of [^{3}H]GABA by the concatemer upon addition of serotonin (up to 1 mM) (Fig. 6B); similarly, GABA caused no significant efflux of [^{3}H]MPP^+ (512 ± 65 and 532 ± 85 cpm efflux under baseline conditions and after addition of 1 mM GABA, respectively).

A Role for Activation of Protein Kinase C. The data summarized above indicate that the local increase in Na^+

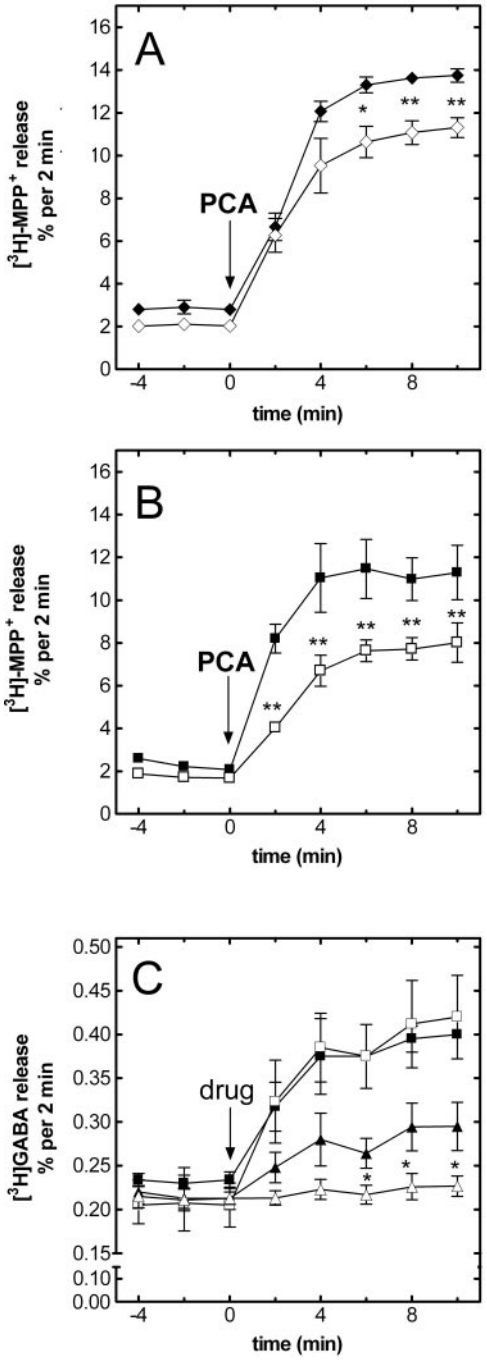

Fig. 7. A role for protein kinase C in PCA-induced efflux. HEK293 cells stably expressing CFP-SERT-YFP (A and B) and CFP-SERT-GAT-1 (C) were preloaded with [^{3}H]MPP^+ (A and B) or [^{3}H]GABA (C) and superfused with buffer as outlined in the legend to Fig. 1B. During the preloading and washout period, the cover slips were incubated in the absence (filled symbols, A–C) or presence of 1 μM GF109203X (open symbols, A and C) or 0.5 μM GÖ 6983 (□, B) and throughout the whole experiment to inhibit protein kinase C. A and B, after three baseline fractions, cells were exposed to PCA (3 μM; ♦, ◊) for five fractions. C, after three baseline fractions, cells were exposed to either GABA (1 mM; ■, □) or PCA (1 mM; ▲, △). The symbols represent means ± S.E.M. of three independent experiments carried out in triplicate; *, $p < 0.05$; **, $p <$ <0.01 compared with the corresponding control.

does not suffice to account for the action of amphetamines. It has been appreciated for some time that, in brain slices, amphetamine-induced transport reversal in the dopamine transporter can—in part—be blunted by the inhibition of protein kinase C isoforms (Kantor and Gnegy, 1998). This effect can also be recapitulated in cells that express CFP-SERT-YFP (Fig. 7A); the efflux of [^{3}H]MPP$^+$ that is induced by 3 μM PCA (Fig. 7A, closed symbols) is significantly reduced in the presence of the protein kinase C inhibitors GF109203X (1 μM; Fig. 7A, open symbols) and Gö6983 (0.5 μM; Fig. 7B, open symbols). Likewise, GF109203X blunted the efflux of [^{3}H]MPP$^+$ through the concatemer that was induced by PCA (data not shown). It is even more noteworthy that GF109203X abolished the PCA-induced outward transport of [^{3}H]GABA (Fig. 7C, compare △ and ▲). In contrast, when tested in parallel on GABA-induced [^{3}H]GABA efflux, inhibition of protein kinase C caused no appreciable change in efflux (Fig. 7C, compare □ and ■). The fact that inhibition of PKC reversed the effect of PCA on the concatemer also indicates that concatemerization does not impair PKC-dependent regulation. At the concentration employed in the release experiments summarized in Fig. 7 (1 μM), GF109203X inhibited neither uptake of PCA (Fig. 2C), uptake of serotonin (Fig. 2D), nor binding of [^{3}H]β-CIT to membranes of cells expressing CFP-SERT-YFP (data not shown). Likewise, Gö6983 did not interfere with inward transport (Fig. 2D, ▼).

Our observations highlight the difference between amphetamine-induced transport reversal and efflux caused by substrate-induced exchange diffusion. In particular, whereas increases in the local internal Na^+ concentration allow for the accumulation of inward-facing conformations, they do not suffice to prime the inward-facing conformations for outward transport of substrate. This is apparently accomplished by the additional action of protein kinase C, which is induced by amphetamines but not by physiological substrates (i.e., serotonin and GABA). This interpretation is supported by a recent report: removal of amino terminal PKC-consensus phosphorylation sites abolishes the amphetamine-induced transport reversal in the dopamine transporter (Khoshbouei et al., 2004). By providing related observations in SERT and GAT-1, our approach generalizes the validity of this concept.

Concomitant versus Sequential Counter-Transport. Our data are best explained by assuming that influx and efflux pathways are located in separate moieties of an oligomeric transporter (Fig. 8A). This double-barrel model postulates concomitant counter-transport rather than the sequential counter-transport predicted from the alternate access model (Fig. 8B). The concomitant counter-transport model accounts for 1) the bell-shaped curve of the amphetamine analogs PCA and MDMA in inducing release of [^{3}H]MPP$^+$ and [^{3}H]5-HT (Fig. 1, B–E, H–I); 2) the ability of PCA (and MDMA) to induce release of [^{3}H]GABA-release through the concatemer (Fig. 6, A–C); and 3) the mutual inhibition of uptake through the concatemer; that is, PCA and MDMA inhibit [^{3}H]GABA uptake and GABA inhibits inward transport of [^{3}H]5-HT (Fig. 5). They cause a localized increase in internal [Na^+] in the very vicinity of the transporter that can be sensed in the concatemer but not by coexpressed transporters.

However, it is evident that this model of concomitant counter-transport fails to explain why the release induced by serotonin results in a monophasic concentration-response

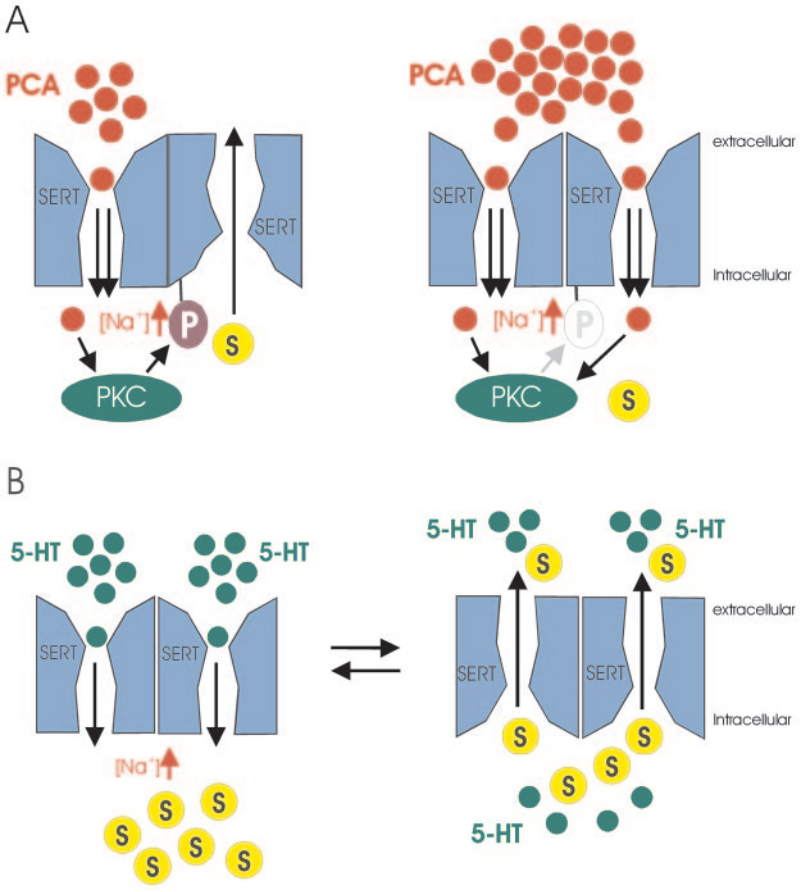

Fig. 8. Schematic illustration of the concomitant and sequential counter-transport models. The differences are depicted in the efflux of intracellular substrate (S) elicited by PCA (A) and 5-HT (B). In A, the left side illustrates the effect of low PCA concentrations; only a fraction of SERT moieties is occupied by PCA in the oligomeric complex (shown here for the sake of simplicity as a dimer). Occupancy by PCA precludes phosphorylation by PKC. The other SERT moieties in the oligomeric complex that has not been occupied by PCA are subject to phosphorylation and thereby primed for outward transport of substrate. Right, at high PCA concentrations, all transporter subunits are occupied by PCA. which impairs the action of PKC and thus prevents the accumulation of inward-facing conformations: efflux of substrate is impaired. B depicts the mechanism of 5-HT-induced sequential outward transport. 5-HT lacks the ability to activate PKC; the observed outward transport of preloaded substrate depends on sequential cycling between inward- and outward-facing conformations (which represents the classic alternate access model; see Jardetzky, 1966). Therefore, a higher occupancy (EC_{50} for serotonin ~ 10 μM; see Fig. 1G) is needed to favor the accumulation of inward facing conformations.

curve, where inhibition is absent at high serotonin concentrations (i.e., 1 mM; see Fig. 1G). In fact, it is worth noting that a substantially higher occupancy (EC_{50} for serotonin ~ 10 μM; see Fig. 1G) is needed to favor the accumulation of inward-facing conformations than with amphetamines (EC_{50} for PCA ~ 0.6 μM; see Fig. 1C) despite their comparable affinities for SERT (the K_M for uptake and K_i for inhibition of β-CIT binding ~ 2 to 3 μM for both PCA and serotonin). Substantially higher local intracellular sodium concentration can be expected at serotonin concentrations that elicit substrate efflux than with the amphetamines. Thus, when challenged by external serotonin, SERT must apparently operate in a sequential counter-transport mode, because reverse transport is seen only at concentrations approaching full occupancy (Fig. 8B). Consistent with this interpretation that serotonin-dependent efflux relies on sequential rather than concomitant counter-transport, serotonin fails to induce release of [^{3}H]GABA through the concatemer (Fig. 6B), although serotonin does inhibit the influx of [^{3}H]GABA through the concatemer (Fig. 5, D and E). We propose that the crucial switch between concomitant and sequential counter-transport is provided by protein kinase C activation.

Transport of substrate per se precludes phosphorylation of SERT (Ramamoorthy and Blakely, 1999; Whitworth et al., 2002). In contrast to serotonin, addition of PCA and MDMA (and other amphetamines) results in activation of PKC (Giambalvo, 1992a,b; Kramer et al., 1998; Giambalvo et al., 2003). If we assumed that PCA and other amphetamines induced release via a sequential mode, it would be difficult to explain the difference between serotonin and the amphetamines, in particular why PCA and MDMA—but not serotonin—have bell-shaped concentration-response curves and why they cause release of [^{3}H]GABA through the concatemer.

Acknowledgments

We thank Drs. H. Betz, J. Bockaert, and U. Gether for critical comments on the manuscript.

References

Abramson J, Smirnova I, Kasho V, Verner G, Kaback HR, and Iwata S (2003) Structure and mechanism of the lactose permease of *Escherichia coli*. *Science (Wash DC)* **301:**610–615.

Adams SV and DeFelice LJ (2003) Ionic currents in the human serotonin transporter reveal inconsistencies in the alternating access hypothesis. *Biophys J* **85:**1548–1559.

Axelrod J, Whitby LG, and Hertting G (1961) Effect of psychotropic drugs on the uptake of ^{3}H-norepinephrine by tissues. *Science (Wash DC)* **133:**383–384.

Caspi A, Sugden K, Moffitt TE, Taylor A, Craig IW, Harrington H, McClay J, Mill J, Martin J, Braithwaite A, and Poulton R (2003) Influence of life stress on depression: moderation by a polymorphism in the 5-HTT gene. *Science (Wash DC)* **301:**386–389.

Chen NH, Reith ME, and Quick MW (2004) Synaptic uptake and beyond: the sodium- and chloride-dependent neurotransmitter transporter family SLC6. *Pflueg Arch Eur J Physiol* **447:**519–531.

Farhan H, Korkhov VM, Paulitschke V, Dorostkar MM, Scholze P, Kudalcek O, Freissmuth M, and Sitte HH (2004) Two discontinuous segments in the carboxy terminus are required for membrane targeting of the rat GABA transporter-1 (GAT1). *J Biol Chem* **279:**28553–28563.

Fischer JF and Cho AK (1979) *Chemical* release of dopamine from striatal homogenates: evidence for an exchange diffusion model. *J Pharmacol Exp Ther* **208:**203–209.

Giambalvo CT (1992a) Protein kinase C and dopamine transport. 1. Effects of amphetamine in vivo. *Neuropharmacology* **31:**1201–1210.

Giambalvo CT (1992b) Protein kinase C and dopamine transport. 2. Effects of amphetamine in vitro. *Neuropharmacology* **31:**1211–1222.

Giambalvo CT (2003) Differential effects of amphetamine transport vs. dopamine reverse transport on particulate PKC activity in striatal synaptoneurosomes. *Synapse* **49:**125–133.

Gobbi M, Moia M, Pirona L, Ceglia I, Reyes-Parada M, Scorza C, and Mennini T (2002) *p*-Methylthioamphetamine and 1-(*m*-chlorophenyl)piperazine, two non-neurotoxic 5-HT releasers in vivo, differ from neurotoxic amphetamine derivatives in their mode of action at 5-HT nerve endings in vitro. *J Neurochem* **82:**1435–1443.

Hahn MK, Robertson D, and Blakely RD (2003) A mutation in the human norepinephrine transporter gene (SLC6A2) associated with orthostatic intolerance disrupts surface expression of mutant and wild-type transporters. *J Neurosci* **23:**4470–4478.

Hastrup H, Karlin A, and Javitch JA (2001) Symmetrical dimer of the human dopamine transporter revealed by cross-linking Cys-306 at the extracellular end of the sixth transmembrane segment. *Proc Natl Acad Sci USA* **98:**10055–10060.

Hastrup H, Sen N, and Javitch JA (2003) The human dopamine transporter forms a tetramer in the plasma membrane: cross-linking of a cysteine in the fourth transmembrane segment is sensitive to cocaine analogs. *J Biol Chem* **278:**45045–45048.

Henderson PJ (1993) The 12-transmembrane helix transporters. *Curr Opin Cell Biol* **5:**708–721.

Horschitz S, Hummerich R, and Schloss P (2003) Functional coupling of serotonin and noradrenaline transporters. *J Neurochem* **86:**958–965.

Huang Y, Lemieux MJ, Song J, Auer M, and Wang DN (2003) Structure and mechanism of the glycerol-3-phosphate transporter from *Escherichia coli*. *Science (Wash DC)* **301:**616–620.

Kramer HK, Poblete JC, and Azmitia EC (1998) Characterization of the translocation of protein kinase C (PKC) by 3,4-methylenedioxymethamphetamine (MDMA/Ecstasy) in synaptosomes: evidence for a presynaptic localization involving the serotonin transporter (SERT). *Neuropsychopharmacology* **19:**265–277.

Jardetzky O (1966) Simple allosteric model for membrane pumps. *Nature (Lond)* **211:**969–970.

Just H, Sitte HH, Schmid JA, Freissmuth M, and Kudlacek O (2004) Identification of an additional interaction domain in transmembrane domains 11 and 12 that supports oligomer formation in the human serotonin transporter. *J Biol Chem* **279:**6650–6657.

Kantor L and Gnegy ME (1998) Protein kinase c inhibitors block amphetamine-mediated dopamine release in rat striatal slices. *J Pharmacol Exp Ther* **284:**592–598.

Khoshbouei H, Sen N, Guptaroy B, Johnson L, Lund D, Gnegy ME, Galli A, and Javitch JA (2004) N-terminal phosphorylation of the dopamine transporter is required for amphetamine-induced efflux. *PLoS Biol* **2:**E78.

Khoshbouei H, Wang H, Lechleiter JD, Javitch JA, and Galli A (2003) Amphetamine-induced dopamine efflux. A voltage-sensitive and intracellular Na^+-dependent mechanism. *J Biol Chem* **278:**12070–12077.

Lesch KP, Bengel D, Heils A, Sabol SZ, Greenberg BD, Petri S, Benjamin J, Muller CR, Hamer DH, and Murphy DL (1996) Association of anxiety-related traits with a polymorphism in the serotonin transporter gene regulatory region. *Science (Wash DC)* **274:**1527–1531.

Langeloh A, Bonisch H, and Trendelenburg U (1987) The mechanism of the ^{3}H-noradrenaline releasing effect of various substrates of uptake1: multifactorial induction of outward transport. *Naunyn- Schmiedeberg's Arch Pharmacol* **336:**602–610.

Pifl C and Singer EA (1999) Ion dependence of carrier-mediated release in dopamine or norepinephrine transporter-transfected cells questions the hypothesis of facilitated exchange diffusion. *Mol Pharmacol* **56:**1047–1054.

Ramamoorthy S and Blakely RD (1999) Phosphorylation and sequestration of serotonin transporters differentially modulated by psychostimulants. *Science (Wash DC)* **285:**763–766.

Rudnick G (1998) Bioenergetics of neurotransmitter transport. *J Bioenerg Biomembr* **30:**173–185.

Schmid JA, Scholze P, Kudlacek O, Freissmuth M, Singer EA, and Sitte HH (2001) Oligomerization of the human serotonin transporter and of the rat GABA transporter 1 visualized by fluorescence resonance energy transfer microscopy in living cells. *J Biol Chem* **276:**3805–3810.

Scholze P, Sitte HH, and Singer EA (2001) Substantial loss of substrate by diffusion during uptake in HEK-293 cells expressing neurotransmitter transporters. *Neurosci Lett.* **309:**173–176.

Scholze P, Freissmuth M, and Sitte HH (2002) Mutations within an intramembrane leucine heptad repeat disrupt oligomer formation of the rat GABA transporter 1. *J Biol Chem* **277:**43682–43690.

Schwartz JW, Blakely RD, and DeFelice LJ (2003) Binding and transport in norepinephrine transporters. Real-time, spatially resolved analysis in single cells using a fluorescent substrate. *J Biol Chem* **278:**9768–9777.

Shannon JR, Flattem NL, Jordan J, Jacob G, Black BK, Biaggioni I, Blakely RD, and Robertson D (2000) Orthostatic intolerance and tachycardia associated with norepinephrine-transporter deficiency. *N Engl J Med* **342:**541–549.

Sitte HH and Freissmuth M (2003) Oligomer formation by Na^+-Cl^--coupled neurotransmitter transporters. *Eur J Pharmacol* **479:**229–236.

Sitte HH, Hiptmair B, Zwach J, Pifl C, Singer EA, and Scholze P (2001) Quantitative analysis of inward and outward transport rates in cells stably expressing the cloned human serotonin transporter: inconsistencies with the hypothesis of facilitated exchange diffusion. *Mol Pharmacol* **59:**1129–1137.

Sitte HH, Huck S, Reither H, Boehm S, Singer EA, and Pifl C (1998) Carrier-mediated release, transport rates, and charge transfer induced by amphetamine, tyramine and dopamine in mammalian cells transfected with the human dopamine transporter. *J Neurochem* **71:**1289–1297.

Sorkina T, Doolen S, Galperin E, Zahniser NR, and Sorkin A (2003) Oligomerization of dopamine transporters visualized in living cells by fluorescence resonance energy transfer microscopy. *J Biol Chem* **278:**28274–28283.

Torres GE, Carneiro A, Seamans K, Fiorentini C, Sweeney A, Yao WD, and Caron MG (2003a) Oligomerization and trafficking of the human dopamine transporter. Mutational analysis identifies critical domains important for the functional expression of the transporter. *J Biol Chem* **278:**2731–2739.

Torres GE, Gainetdinov RR, and Caron MG (2003b) Plasma membrane monoamine transporters: structure, regulation and function. *Nat Rev Neurosci* **4:**13–25.

Whitworth TL, Herndon LC, and Quick MW (2002) Psychostimulants differentially regulate serotonin transporter expression in thalamocortical neurons. *J Neurosci* **22:**RC192.

Address correspondence to: Dr. Michael Freissmuth, Institute of Pharmacology, Medical University Vienna, Währinger Str. 13a, A-1090 Vienna, Austria. E-mail: michael.freissmuth@meduniwien.ac.at